ISSN (Print) 1226-5268 ISSNS (Online) 2287-7169
The Journal of Engineering Geology, Vol.25, No.1, March, 2015, pp. 1-8
http://dx.doi.org/10.9720/kseg.2015.1.1

Effects of Temperature and Pressure on Quartz Dissolution

Jung-Hae Choi*, Byung-Gon Chae, and Hye-Jin Kim

Geologic Environment Division, Korea Institute of Geoscience and Mineral Resources

Received 6 January 2015; received in revised form 4 March 2015; accepted 9 March 2015

Deep geological disposal is the preferred storage method for high-level radioactive waste, because it ensures stable long-term storage with minimal potential for human disruption. Because of the risk of groundwater contamination, a buffer of steel and bentonite layers has been proposed to prevent the leaching of radionuclides into groundwater. Quartz is one of the most common minerals in earth's crust. To understand how deformation and dissolution phenomena affect waste disposal, here we study quartz samples at pressure, temperature, and pH conditions typical of deep geological disposal sites. We perform a dissolution experiment for single quartz crystals under different pressure and temperature conditions. Solution samples are collected and the dissolution rate is calculated by analyzing Si concentrations in a solution excited by inductively coupled plasma-atomic emission spectroscopy (ICP-AES). After completing the dissolution experiment, deformation of the quartz sample surfaces is investigated with a confocal laser scanning microscope (CLSM). An empirical formula is introduced that describes the relationship between dissolution rate, pressure, and temperature. These results suggest that bentonite layers in engineering barrier systems may be vulnerable to thermal deformation, even when exposed to higher temperatures on relatively short timescales.

Key words: deep geological disposal, quartz dissolution, dissolution rate, CLSM

Introduction

Global energy demand has substantially increased due to recent population growth and economic development, but energy resources are relatively limited. In particular, fossil fuels such as coals or oils may be exhausted soon. Nuclear power generation is an increasingly popular solution to this problem, due to its high energy efficiency, relatively easy reservation, and lack of contribution to greenhouse gas emissions. However, nuclear power produces high-level radioactive waste that can adversely affects human health and ecosystems, even in small quantities. Many high-level radionuclides have long half-lives. Thus, waste isolation can be necessary for a period ranging from tens of thousands of years to almost one million years.

Although many methods have been proposed for high-level waste disposal, deep geological disposal is most powerfully mentioned. This technique dissolves high-level radioactive waste by mixing it in glass, then disposing of the vitrified waste forms by burial in a stable geologic setting. Due to the need for intermediary containment, vitrified waste forms are typically enclosed in an overpack of steel and stored in cooled facilities at 300-1000 m below the surface. Although many additional engineer barrier systems (EBS) have been proposed to further isolate waste, an increasingly popular EBS configuration is an overpack of steel and bentonite.

*Corresponding author: jhchoi@kigam.re.kr

The goal of such systems is to completely isolate radioactive materials by using artificial materials. Because deep geological disposal sites are typically 300-1000 m below the surface, earthquakes and human activities have less of an impact than at shallow sites. However, a number of studies suggest that poorly designed casings can lead to the leaching of radioactive waste into groundwater. Bentonite is being considered as a buffer material because its low permeability and high absorbency inhibit groundwater flow. Because bentonite infiltrates cracks in the bedrock, it is thought to increase the long-term viability of deep storage facilities. In addition, as bentonite has a very high amount of exchangeable cations, it inhibits radionuclide leaching by absorbing radionuclides consisting of cations. Therefore, bentonite has favorable properties for isolating high-level radioactive waste.

Because quartz accounts for a high proportion of the macro materials in bentonite, the physical and chemical properties of quartz can serve as a proxy for investigating long-term stability of bentonite casings in this study, experiments are carried out under various pressures and temperatures to study quartz deformation at depths of 300-1000 m below the surface. Empirical formulae for dissolution rates are derived for the purpose of investigating bentonite stability at depths where high-level radioactive waste disposal facilities might be constructed.

Quartz dissolution and controlling factors

The dissolution of quartz begins with the absorption of a water molecule by surficial Si. H^+ from the water molecule then bonds with Si and O to form Si-OH. Through these reactions, a total of 4 H^+ ions interact with Si-O and then one molecule of H_4SiO_4 is produced. The surface of the quartz begins to dissolve after the H_4SiO_4 separates. The dissolution phenomenon has been known to occur rapidly because the opportunities for surface H^+ absorption increase when pore pressure increases (Gratz and Bird, 1993; Anzalone et al., 2006).

The dissolution behavior of quartz by sequential reactions involving quartz and water can be expressed as follows:

$$\begin{aligned}
&H_2O + \equiv Si - \underset{}{\overset{K_1}{\rightleftharpoons}} H_2O_{ads} \cdot Si \xrightarrow{k_1} \equiv Si\text{-}OH,\\
&H_2O + \equiv Si\text{-}OH \overset{K_2}{\rightleftharpoons} H_2O_{ads} \cdot Si\text{-}OH \xrightarrow{k_2} =Si(OH)_2,\\
&H_2O + =Si(OH)_2 \overset{K_3}{\rightleftharpoons} H_2O_{ads} \cdot Si(OH)_2 \xrightarrow{k_3} -Si(OH)_3,\\
&H_2O + -Si(OH)_3 \overset{K_4}{\rightleftharpoons} H_2O_{ads} \cdot Si(OH)_3 \xrightarrow{k_4} H_4SiO_{4,ads},\\
&H_4SiO_{4,ads} \xrightarrow{k_5} H_4SiO_4(aq).
\end{aligned} \tag{1}$$

where *ads* represents an adsorption state, *aq* represents a dissolution state, K_i is the equilibrium constant for the adsorption of H_2O to SiO_2, and k_i is the reaction constant (Bennett et al., 1988; Brady and Walther, 1989; Brady and Walther, 1990).

Effects of temperature

The effect of temperature on dissolution rate is expressed by the Arrhenius equation (Bennett, 1991):

$$k_+ = Ae^{-E_a/RT} \tag{2}$$

where k_+ is the forward rate constant, A is the pre-exponential factor, E_a is the activation energy, R is the gas constant, and T is absolute temperature in Kelvin (Bennett, 1991). The activation energy E_a is produced through the entire reaction. When dissolution is repeated over a range of temperatures, the activation energy can be obtained by fitting a straight line to a plot of $1/T$ vs. ln k (Fig. 1). On the graph, the y-intercept is ln A, and E_a can be calculated from the slope.

Effects of pH

When temperature is held constant, the proton (H^+) and

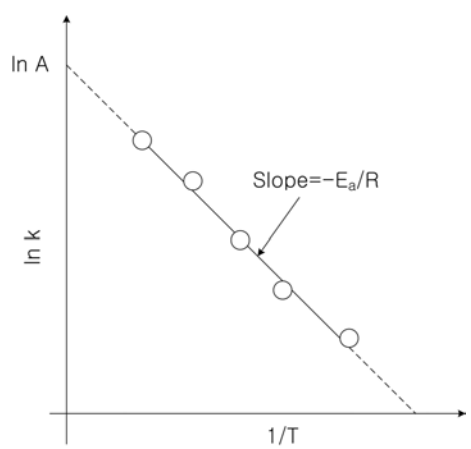

Fig. 1. Arrhenius plot.

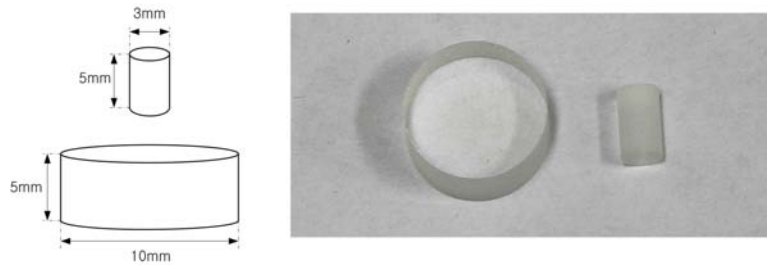

Fig. 2. Schematic figure and photograph of sample specimens.

hydroxyl group (OH^-) play the most important role in altering the surface of minerals. The relationship between concentration and dissolution rates can be expressed as

$$R = k_a \cdot [H^+]^n$$
$$R = k_h \cdot [OH^-]^m \quad (3)$$

where R is the dissolution rate; k_a and k_b are rate constants for the acid and base in the pH range, respectively; [·] is the concentration of each ion; and n and m are the reaction order (Berger et al., 1994; Bickmore et al., 2006), which can be calculated from the slope of the best-fit line for logR as a function of pH.

Effects of pressure

The pressure dissolution phenomenon consists of three specific processes: the dissolution phenomenon of constituent particles on the contact surface, the diffusion of dissolved materials, and the reprecipitation on the free surface between particles. The dissolution mass flux for the contact surface is given by

$$\frac{dM_{diss}}{dt} = \frac{3\pi V_m^2(\sigma_a - \sigma_c)k^* \rho g d_c^2}{4RT} \quad (4)$$

where V_m is the molar volume, σ_a is the contact surface stress, σ_c is the critical stress, k^* is the dissolution rate constant, ρg is the particle density, d_c is the diameter of the contact between particles, R is the gas constant, and T is absolute temperature (Tada et al., 1987). Dissolution mass flux thus represents the amount of material dissolution on the contact surface per unit time. From the equation, the dissolution rate is affected by pressure and temperature.

Quartz dissolution experiments and analysis method

Samples and experiment device

Two kinds of cylindrical samples with different sizes were produced and used in this research (Fig. 2).

In this experiment, two samples were in contact and high pressure was applied to the contact area. A loading device was placed in an oven with the temperature preset to either 40°C or 80°C. An NaOH solution was added to an inlet tank installed outside the oven, with p set to 11.7 to reproduce the expected conditions of a deep underground facility. The NaOH solution was added to an Inlet tank installed outside the oven, where it could not be affected by the oven temperature. The oven and inlet tank were sealed to minimize changes in pH due to contact with outside air. After the injected NaOH solution passed through the sample, it was removed by a peristaltic pump at an extraction rate of 0.15 ± 0.05 ml/h. A weight system was configured to apply pressures of 7.33 MPa or 19.5 MPa to the contact surfaces of the two samples. Fig. 3 shows a schematic figure and photographs of the instrumental setup.

Confocal laser scanning microscope (CLSM) analysis

A confocal laser scanning microscope (CLSM) was used to observe dissolution phenomenon and the surface deformation of samples after the dissolution experiment (Fig. 4). The CLSM can create a three-dimensional image by utilizing a laser with a wavelength of 420 nm. In this case, the three-dimensional image was created by combining two-dimensional images taken at several μm (minimum of 0.01 μm) for the lowest point and highest

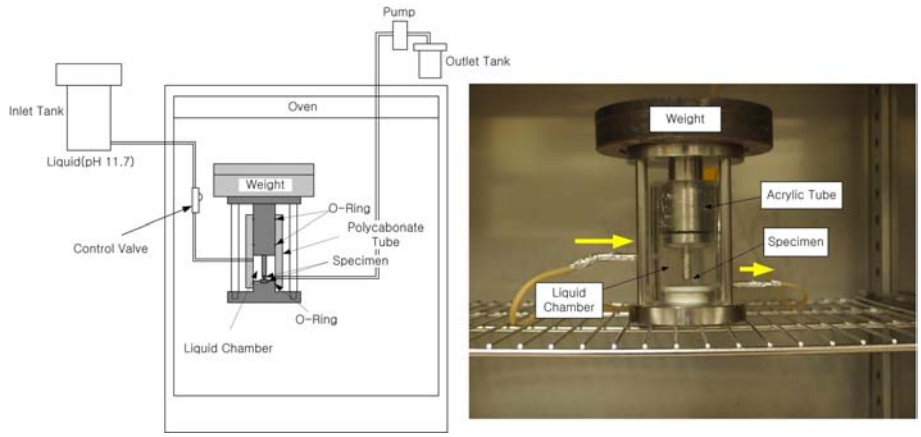

Fig. 3. Schematic figure and photograph of the experimental setup.

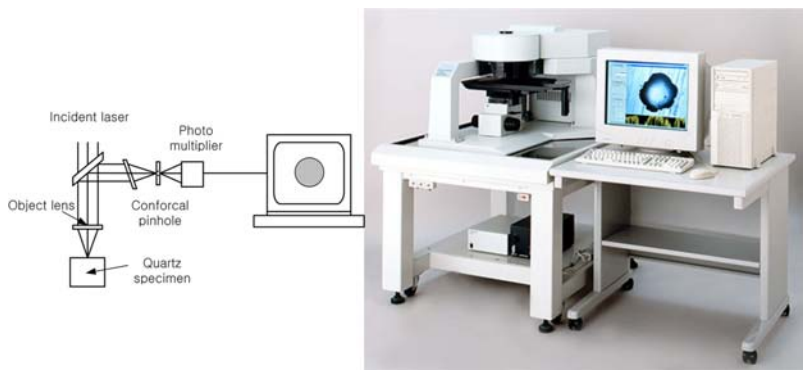

Fig. 4. Confocal microscopy using a pinhole shape (left) and photograph (right) of the CLSM.

point in the scanned region. Because the CLSM aperture has a pinhole shape, areas ranging from the lowest point to the highest point could be imaged in three dimensions by adjusting the focus to the appropriate height. Given that all of the acquired images are 1024 × 1024 pixels in size, the sample area represented by each pixel was calculated, and numerical values were directly expressed (Choi and Chae, 2012).

Analysis of Si concentrations using emission spectroscopy

Inductively coupled plasma-atomic emission spectroscopy (ICP-AES) elevates the energy levels of the component elements in a solution by applying plasma energy to samples from the outside. When excited electrons return to the ground state, spectral lines are produced at specific wavelengths whose intensities give the relative concentrations of each element. A high-density, high-temperature (10,000 K) plasma is generated by ionizing argon gas in a

Fig. 5. ICP-AES (Vista-PRO).

torch tube, and the electromagnetic field produced by a high-frequency current is applied to a work coil. The plasma is then used to elevate the energy level of the sample.

In this study, we used a SEICO Vista-PRO spectrometer. The apparatus for this phase of the analysis is shown in Fig. 5. A solution sample was introduced into the gasified plasma through a thin tube in the central torch tube. ICP-AES equipment requires sample pre-treatment, but is characterized by precise relative measurements of trace elements.

Results and discussion

CLSM surface analysis

The surface pattern of a sample is shown in Fig. 6. The left panels show the result of applying a contact surface pressure of 19.5 MPa at a temperature of 80°C. The right panels show the result for a contact surface pressure of 7.33 MPa at 80°C. Black areas in the figure represent recessed points (negative height anomaly) and white areas represent protruding points (positive height anomaly). In the upper panels in Fig. 6, thick dark strips appear at the grain boundary of a small quartz crystal located in the top part of the sample. Thus, this pattern is thought to be the characteristic shape of the dissolution phenomenon. In addition, these two cases show higher points around the black regions in a three-dimensional figure. Fig. 7 shows a cross-section through the sample after the experiment. Dissolved materials are repreicpitated in free space and the dissolved part can be distinguished from the reprecipitated part.

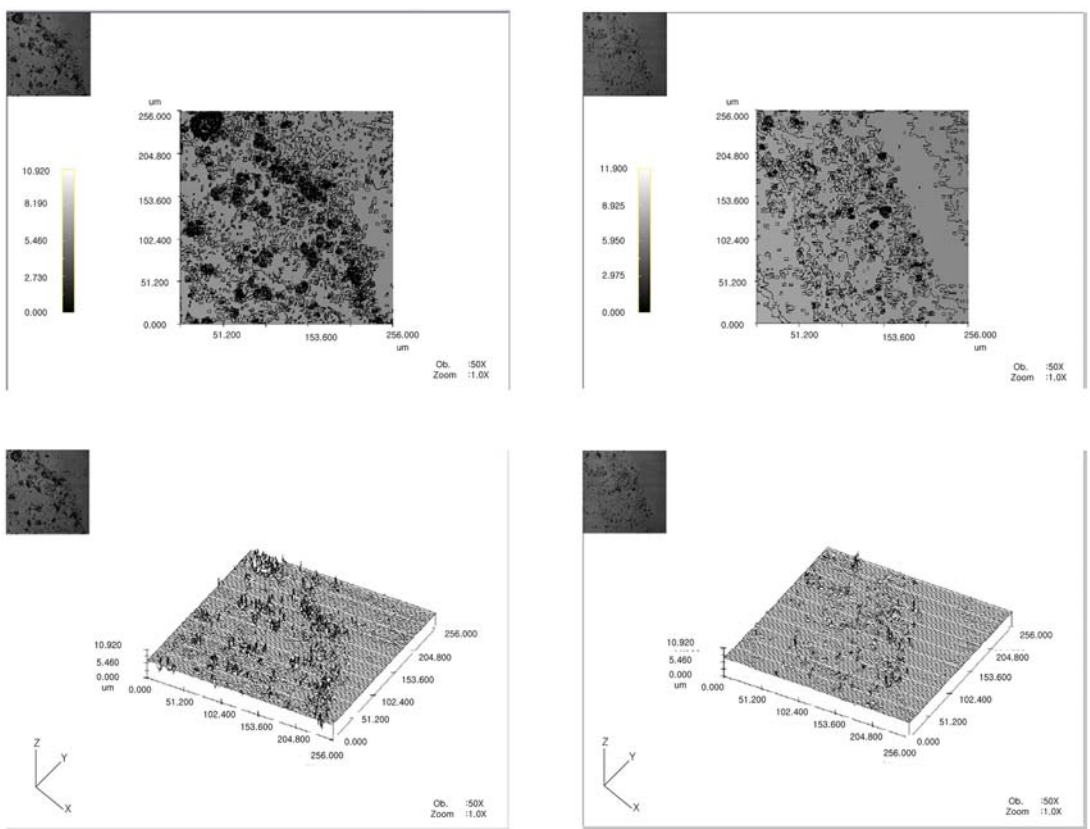

Fig. 6. 2D and 3D images of specimen subsurfaces after treatment at 19.5 MPa, 80°C (left panels) and 7.33 MPa, 80°C (right panels). Black areas represent lower points (negative height anomaly) and white areas represent higher points (positive height anomaly).

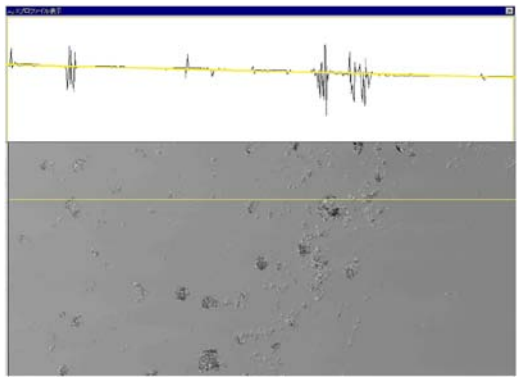

Fig. 7. Digital profile image of a specimen after treatment (19.5 MPa). Characteristic spatial signatures of dissolution are evident in the middle part of the image.

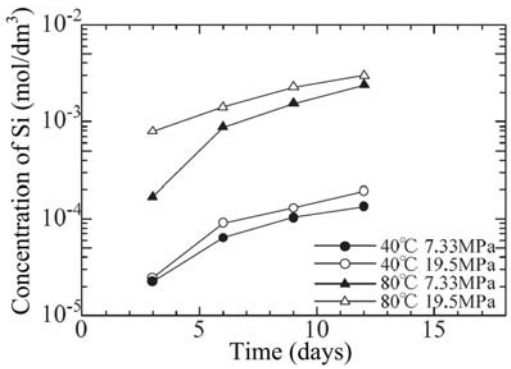

Fig. 8. Accumulated concentration of Si (C_{Si}) in the tested solutions according to elapsed time under various temperatures and pressures.

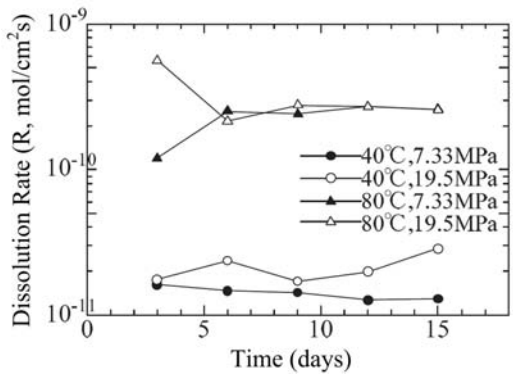

Fig. 9. Dissolution rate vs. time for various temperatures and pressures.

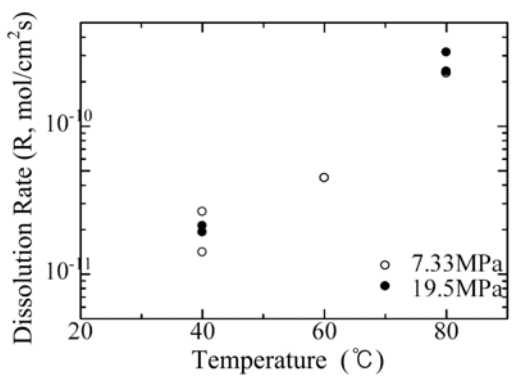

Fig. 10. Dissolution rate vs. temperature.

Calculation of the dissolution rate from ICP-AES analyses

In the present experiment, pressures of 7.33 MPa and 19.5 MPa are applied to the contact surface at temperatures of 40°C and 80°C, giving a total of four possible pressure-temperature regimes. Results are compared after 15 days of continuous exposure to these temperatures and pressures. The cumulative concentration of Si over time is calculated and concentrations are determined at each time point. The dissolution rate over time and the final dissolution rate are obtained using the above concentrations. The Si concentration at each time point is also calculated. The amount of the substance is then calculated from the volume of Si dissolved in the cumulative concentration of Si (C_{si}). The dissolution rate at each time point and the final dissolution rate are then calculated by dividing the result by the surface area and contact time for the surface.

Fig. 8 shows the calculated dissolution rates. The cumulative concentration of Si is much higher at high temperature than at low temperature, even under the same pressure. In addition, the Si concentration under high pressure is higher than that under low pressure at the same temperature. Fig. 9 shows the dissolution rate over time. The dissolution rate tends to sharply increase once the experiment starts, then increases more gradually from the 6th day onward. This is caused by a rapid increase or decrease in dissolution phenomena during the first 6 days, followed by a gradual decrease in the dissolution rate. In addition, it is significant that the dissolution rate is not substantially affected by a pressure difference of 12.17 MPa. This indicates that changes in pressure do not substantially affect the dissolution of quartz, but changes in temperature do.

Fig. 10 shows dissolution rates as a function of applied

pressure. The dissolution rate is more sensitive to changes in temperature than to changes in pressure.

Using these results, we can construct equations that describe the empirical dissolution rate:

$$\ln R = 0.0697T\ (°C) - 27.9\ (7.33\ MPa) \quad (5)$$

$$\ln R = 0.0675T\ (°C) - 27.3\ (19.5\ MPa) \quad (6)$$

$$\ln R = 0.0337\ (MPa) - 25.2\ (40°C) \quad (7)$$

$$\ln R = 0.0269\ (MPa) - 22.4\ (80°C) \quad (8)$$

Discussion and conclusions

This study aimed to analyze the dissolution characteristics of quartz at depths of 300-1000 m below the surface, where high-level radioactive wastes are expected to be stored. A single-crystal dissolution experiment was conducted over 15 days under four combinations of pressure and temperature conditions, with pH fixed at 11.7.

A key result of this study is that the rate of dissolution increases rapidly with temperature, even when pressure is held constant. The difference between the low- and high-temperature dissolution rate is as large as 10^2. This suggests that subtle changes in temperature have a large effect on the dissolution of quartz. In addition, it is suggested that pressure has little or no effect on the dissolution of mineral quartz at high temperatures. These results are supported by the results of CLSM and ICP-AES analyses.

The cumulative concentration of Si changed rapidly during the first 6 days of the experiment. However, the rate of dissolution then decreased, resulting in slowly increasing or even steady cumulative concentrations. This means that dissolution occurred rapidly during the initial stage, but slowed thereafter.

We have quantitatively evaluated the effects of pressure and temperature on the dissolution rate of quartz. Of note, changes in pressure do not significantly affect the dissolution rate, yet even small changes in temperature cause a substantial change. The results indicate that quartz in bentonite may undergo thermal deformation in deep geological disposal sites as a result of long-term exposure to radioactive waste, even if pressure at the disposal sites is held constant. Therefore, this study provides a basic empirical constraint on the viability of bentonite layers in bentonite-steel type engineered barrier systems.

Acknowledgements

This research was supported by the Basic Research Project (Technology Development of Landslide Rapid Detection Based on a Real-Time Monitoring) of the Korea Institute of Geoscience and Mineral Resources (KIGAM), funded by the Ministry of Science, ICT and Future Planning of Korea.

References

Anzalone, A., Boles, J., Green, G., Young, K., Israelachvili, J., and Alcantar, N., 2006, Confined fluids and their role in pressure solution, Chemical Geology, 230(3-4), 220-231.

Bennett, P. C., 1991, Quartz dissolution in organic-rich aqueous systems, Geochimica et Cosmochimica Acta, 55(7), 1781-1797.

Bennett, P. C., Melcer, M. E., Siegel, D. I., and Hassett, J. P., 1988, The dissolution of quartz in dilute aqueous solutions of organic acids at 25°C, Geochimica et Cosmochimica Acta, 52(6), 1521-1530.

Berger, G., Cadore, E., Schott, J., and Dove, P. M., 1994, Dissolution rate of quartz in lead and sodium electrolyte solutions between 25 and 300°C: Effect of the nature of surface complexes and reaction affinity, Geochimica et Cosmochimica Acta, 58(2), 541-551.

Bickmore, B. R., Nagy, K. L., Gray, A. K., and Brinkerhoff, A. R., 2006, The effect of $Al(OH)_4^-$ on the dissolution rate of quartz, Geochimica et Cosmochimica Acta, 70(2), 290-305.

Brady, P. V. and Walther, J. V., 1989, Controls on silicate dissolution rates in neutral and basic pH solutions at 25, Geochimica et Cosmochimica Acta, 53(11), 2823-2830.

Brady, P. V. and Walther, J. V., 1990, Kinetics of quartz dissolution at low temperatures, Chemical Geology, 82, 253-264.

Choi, J. H. and Chae, B. G., 2012, Experimental study on the deformation and failure behavior of Tono granite, The Journal of Engineering Geology, 22(2), 173-183 (in Korean with English abstract).

Gratz, A. J. and Bird, P., 1993, Quartz dissolution: Theory of rough and smooth surfaces, Geochimica et Cosmochimica Acta, 57(5), 977-989.

Tada, R., Maliva, R., and Siever, R., 1987, A new mechanism for pressure solution in porous quartzose sandstone, Geochimica et Cosmochimica Acta, 51(9), 2295-2301.

Jung-Hae Choi
Geologic Environment Division, Korea Institute of Geoscience and Mineral Resources, 124 Gwahak-ro, Yuseong-gu, Daejeon 305-350, Korea
Tel: 042-868-3944
E-mail: jhchoi@kigam.re.kr

Byung-Gon Chae
Geologic Environment Division, Korea Institute of Geoscience and Mineral Resources, 124 Gwahak-ro, Yuseong-gu, Daejeon 305-350, Korea
Tel: 042-868-3052
E-mail: bgchae@kigam.re.kr

Hye-Jin Kim
Geologic Environment Division, Korea Institute of Geoscience and Mineral Resources, 124 Gwahak-ro, Yuseong-gu, Daejeon 305-350, Korea
Tel: 042-868-3944
E-mail: hjkim_91@knu.ac.kr